This journal is © The Royal Society of Chemistry 2018

ESI

Instabilities in the electric Freedericksz state of the twist-bend nematic liquid crystal CB7CB

Kanakapura S. Krishnamurthy,*[a] Madhu B. Kanakala,[a] Channabasaveshwar V. Yelamaggad[a] and Maurice Kleman[b]

[a]*Centre for Nano and Soft Matter Sciences†, P. O. Box 1329, Jalahalli, Bangalore 560013, India. E-mail: murthyksk@cens.res.in*

[b]*Institut de physique du globe de Paris,Université Sorbonne Paris Cité, 1 rue Jussieu, 75238, Paris cédex 05, France*

A. Toric focal conic nuclei in motion

The appearance of a drifting TFC nucleus with its birefringent trail does differ from that of the stationary TFCD. In the former case, the distortion in the axisymmetric nucleus is modulated by the distortion in the trail where the two come to meet. Secondly, with focussing distance, the appearance of the domains changes; these are illustrated in the textures in Fig. A1.

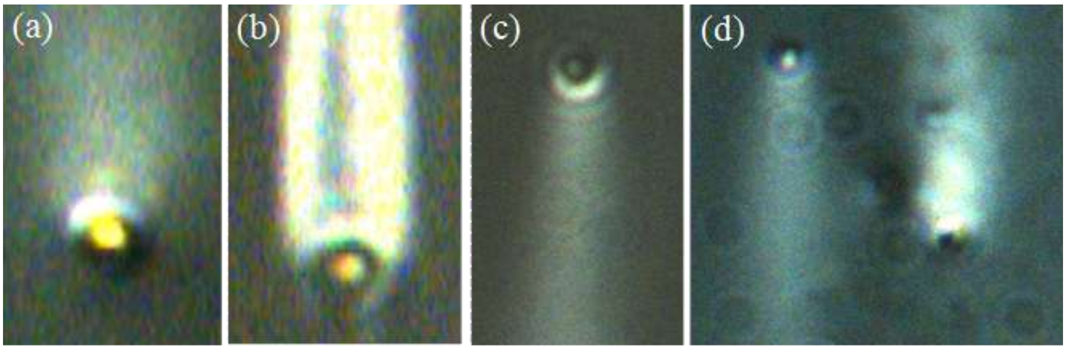

Fig. A1. TFC nuclei vary in appearance with their distance relative to the objective. In (a), the lower part of the dark ring around the bright centre is clearly seen. In (b), the upper part of the dark ring is better defined. In (c), as also in (b), the full dark circle is discernible. In (d), the centre is bright for the nucleus to the left, but dark for the one to the right.

Once the nuclei develop into larger domains, their symmetry is readily seen as in Fig. A2. Thus it seems reasonable to suppose the drifting nuclei as essentially the toric focal conic germs.

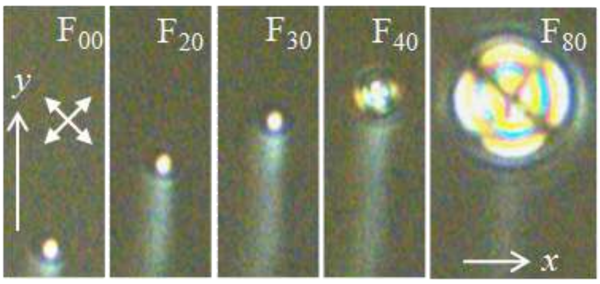

Fig.A2. Time lapse recordings showing the growth of TFC nucleus upon reducing the voltage. F_i is the ith frame of the series. Around F_{20}, U was decreased from 20 V to 8 V, the frequency being 10 kHz. $\Delta T=0.6\ ^{o}C$. Double arrows indicate crossed polarizers.

B. Details of video clips

1. V1.avi is from a time series recorded during the cooling of a 20-μm-thick, initially planarly aligned layer of CB7CB from the splay-Freedericksz N state into the homeotropic N_{TB} state. The sample subjected to a sine wave field (15 V, 1 kHz) is held between diagonally crossed polarizers. The onset of the N_{TB} phase is marked by total extinction of light. The video runs at 10 fps, the original frame rate being 4.13 fps.

2. V2.avi is from a time series showing the instabilities excited by a SQW field (8.9 V, 0.1 Hz) in a 10 μm thick CB7CB layer in a 90$^{\mathrm{o}}$-twist cell held between crossed polarizers, P(0)-A(90). We see here, from left to right, N, N_{x} and N_{TB} regions formed under a slight temperature gradient. The intermediate region is presumably a N-N_{TB}-N sandwich. The video runs at 5 fps compared to the original frame rate of 2.16 fps.

3. V3.avi is from a time series, running at 5 fps, the original frame rate being 0.1 fps. It shows the course of Freedericksz transition in an initially planar 9-μm-thick layer of CB7CB at ~0.2 $^{\mathrm{o}}$C below the setting point, subjected to a sine wave field of frequency 1 kHz and rms voltage 16 V. Polarizer axis is nearly along the rubbing direction and the analyser axis normal to it.

In this video, the dielectric reorientation nucleates at the periphery, which is the high temperature region. It propagates not radially but transversely to the rubbing direction, and oppositely in the upper and lower semicircular halves. This would indicate anisotropic material parameters as more important than the temperature gradient in this heterogeneous progressive transformation.

4. V4.avi is from a time series showing continued dissociation of a TFCD in a planar 20 μm thick layer between axially crossed polarizers, P(0)-A(90); this leads to the formation of a chain of PFCDs. The video is recorded after reducing the voltage from 10 V to 1 V at 1 kHz. It runs at 20 fps, the original frame rate being 2.16 fps.

5. V5.avi, from time lapse recordings, runs at 6 fps, the original frame rate being 2.8 fps. It demonstrates the slight inclination of stripes relative to the y-axis (normal to the rubbing direction x) under the action of a strong dc field. The field switches from –3.5 V/μm to + 3.5 V/μm where the previously formed stripes get suppressed and the field of view turns transiently dark. Subsequently, stripes with opposite inclination nucleate and develop. d=20 μm.

C. The extended Volterra process defect classification: A reminder

Consider a closed loop L traced in a perfect ordered medium; how to create along L a defect characterized by a Burgers vector $\mathbf{b}$ and Frank vector $\boldsymbol{\Omega} = \Omega\mathbf{t}$? The vectors $\mathbf{b}$ and $\boldsymbol{\Omega}$ are translation and rotation symmetries of the medium. The Volterra process[1,2] consists in opening a void of extent

$$\mathbf{d}(\mathbf{M}) = \mathbf{b} + 2\sin \Omega/2\ \mathbf{t} \times \mathbf{OM}$$

along a so-called cut surface S bordered by L, and filling it with perfect matter, then letting this assembly relax elastically. $\mathbf{O}$ is an origin chosen on the axis of rotation $\mathbf{t}$ and $\mathbf{M}$ is a variable point on S. For simplicity, we consider a void; it can as well be a region of double occupation of matter. Because of the 'perfect' (from a symmetry point of view) nature of the Burgers vector **b** and the Frank vector 2sin Ω/2 **t**, this operation can be achieved in such a way that the local ordering is re-established along the two lips S^+ and S^- of S. Thus the singularities are restricted to the line L and its vicinity (the core of the defect).

Whereas the *dislocation* part **b** of the process does not raise specific problems, as long as |**b**| is small, e.g., comparable to molecular dimensions, the *disclination* part 2sin Ω/2 **t** x **OM** can yield large displacements **d**(**M**) on L, if **Ω** is somewhat far from the disclination line; the elastic approximation breaks down in a large zone, the process becoming unphysical. What in reality happens is that the rotation axis is no longer invariable, but has a copy at each point of the line. This does not bring any change to the Volterra process if the line is straight and along **Ω** (a wedge disclination line). But consider a curved disclination, as in Fig. 1(a). Assume first that the

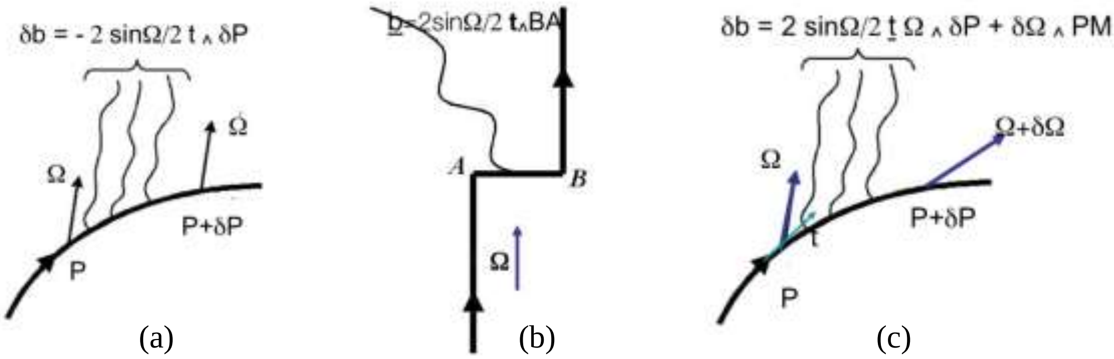

Fig. C1 (a) Infinitesimal dislocations attached along the curvature of a disclination line. (b) Dislocation attached to a kink on a disclination. The length of the kink and the Burgers vector are related in size and position. (c) Infinitesimal dislocations and disclinations attached along a disclination line. Adapted from Kleman et al.[3]

Frank vector is located in **P**: the displacement of the cut surface in $\mathbf{M} \in S$ is $\mathbf{d}(\mathbf{M})|_P$ = 2sin Ω/2 **t** x **PM**. Assume now that a similar rotation vector is also located in $\mathbf{P}' = \mathbf{P} + \delta\mathbf{P}$, the displacement of the cut surface in $\mathbf{M} \in S$ is $\mathbf{d}(\mathbf{M})|_{P'}$ = 2sin Ω/2 **t** x **P′M**. Notice that the difference

$$\mathbf{d}(\mathbf{M})|_{P'} - \mathbf{d}(\mathbf{M})|_P = 2\sin \Omega/2\ \mathbf{t} \times \mathbf{P'P}$$

does not depend on **M**. The displacements of the cut surface viewed from **P** and **P′** differ by a constant vector

$$\delta\mathbf{b} = 2\sin \Omega/2\ \mathbf{t} \times \mathbf{P'P}.$$

Thus if **P** and **P′** are both locations for rotation vectors **Ω**, there is an infinitesimal dislocation of Burgers vector δ**b** attached between **P** and **P′**.

This is the essence of the extended Volterra process. Notice at this point that the infinitesimal dislocation here introduced must be 'perfect' in the sense we have given to this qualifier above, if we require that the lips of the cut surface suffer no singularity: δ**b** has to be a symmetry of translation of the perfect medium.

Such translational symmetries are frequent in liquid crystals. This is true of any translation in an ordinary nematic and of the translations parallel to a quasilayer in the N_{TB} phase.

The same analysis applies to an attached quantized dislocation, i.e., of finite Burgers vector **b**; in this case, the disclination line has a kink at the position of attachment (see Fig. 1(b)). Again **b** must be a symmetry of translation of the medium.

If **Ω** is variable in orientation and/or length along the line, a similar analysis shows that infinitesimal disclinations can be attached to disclinations (see Fig. 1(c)). Again, δ**Ω** has to be an infinitesimal perfect rotation vector.

Finally, attached *infinitesimal dispirations* can exist if there are continuous screw symmetries. This is the case for the N_{TB} phase. Again, the case of quantized dispirations attached to disclinations can possibly exist.

The extended Volterra process approach insists on geometrical properties of defects more than on topological properties. In a sense it is complementary to the topological approach, not presented here. The continuous symmetries, not considered in the topological approach, play a role in the static and dynamical properties of the quantized defects; the corresponding infinitesimal defects act in the viscous relaxation of the medium (e.g., in a liquid crystal).[2]

References

1. J. Friedel, *Dislocations*, Pergamon Press, Oxford, 1964.

2. M. Kleman and J. Friedel, *Rev. Mod. Phys*., 2008, **80**, 61.

3. M. Kleman, O. D. Lavrentovich and Y. A. Nastishin, in *Dislocations in Solids*, ed. F. R. N. Nabarro and J. P. Hirth, Elsevier, Amsterdam, The Netherlands, 2004, Vol. 12, pp. 147–271.

D. Natural textures of the N_{TB} phase of CB7CB in a planar cell, in the absence of any external field

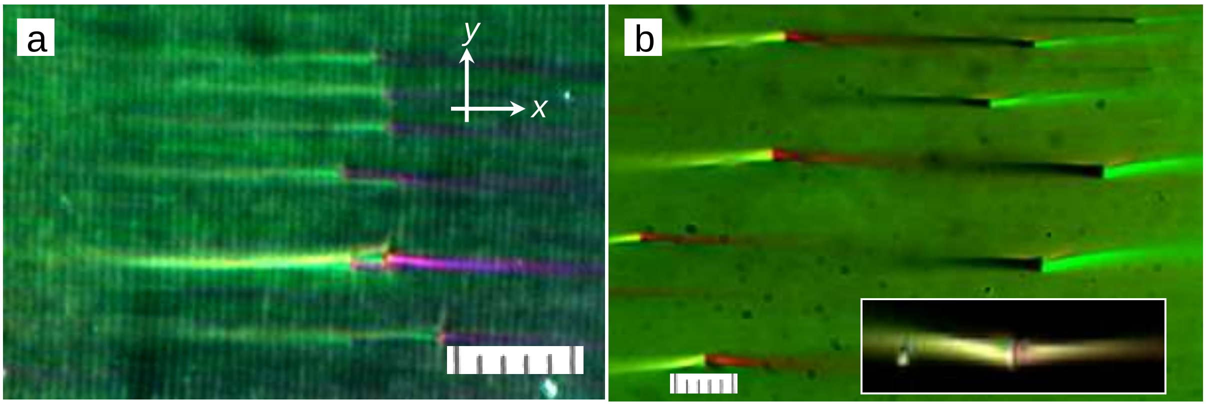

Fig. D1. *(a) At the transition into the N_{TB} state from the planar N state, a pattern of narrow and periodic vertical stripes is observed. (b) On cooling down marginally, the periodic pattern disappears and the texture of "twin-stripes" is seen; the two stripes in each unit meet at a slight angle and, as the inset shows, a loop defect is seen at the junction.*[1] *Presumably, the loop represents the elliptic singularity of the FCD structure, in the yz-plane; and the stripes are due to distortions associated with the confocal hyperbola in the layer plane. Polarizer-Analyzer settings relative to x: (a) P(0)-A(90) and (b) P(0)-A(70). Scale: 5 µm/div.*

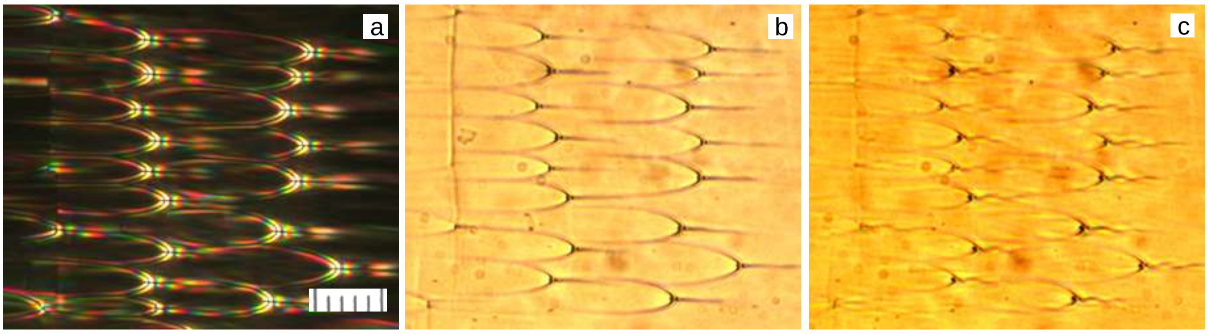

Fig. D2. *Texture of the* N_{TB} *phase on further cooling (~0.3* ^{o}*C relative to* T_s*) from the state represented by Fig. 1b. This is usually interpreted as the parabolic focal conic texture, although the singular line in the layer plane often appears as an incomplete ellipse. The wavy lines at the vertices in (c) are a novel feature. Polarizer-Analyzer settings: (a) P(0)-A(90), (b) P(0) and (c)P(45). Scale: 5* μ*m/div.*

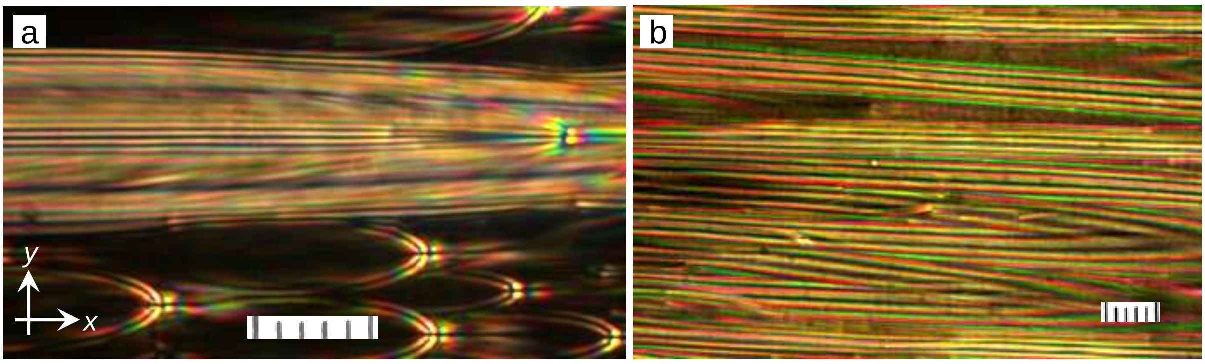

Fig. D3. *The* N_{TB} *phase of CB7CB at 102.4* ^{o}*C showing stripes extending predominantly along x without regular spacing or uniformity of birefringence colour, arising from the focal conic distortion. d=20* μ*m. (P(0)-A(90). Scale: 5* μ*m/div.*

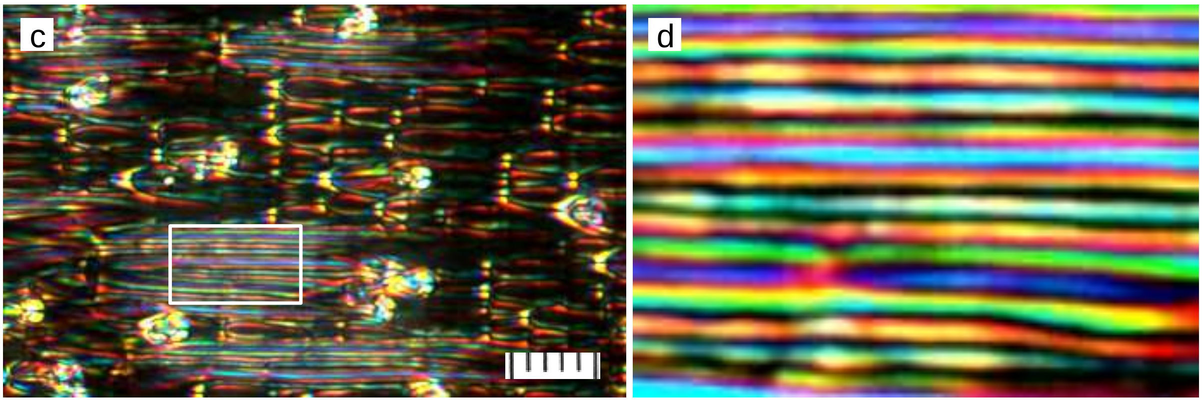

Fig. D3 (contd.). *(c) The* N_{TB} *phase in a bent core compound (4-cyanoresorcinol bis[4-(4-n-hexyloxybenzoyloxy)benzoate) doped with 10% (by weight) of CB7CB, in a planar cell with d=7.7* μ*m; 64* ^{o}*C. (d) Five-fold enlargement of the area within the rectangle in (c). (P(0)-A(90). Scale: 5* μ*m/div.*

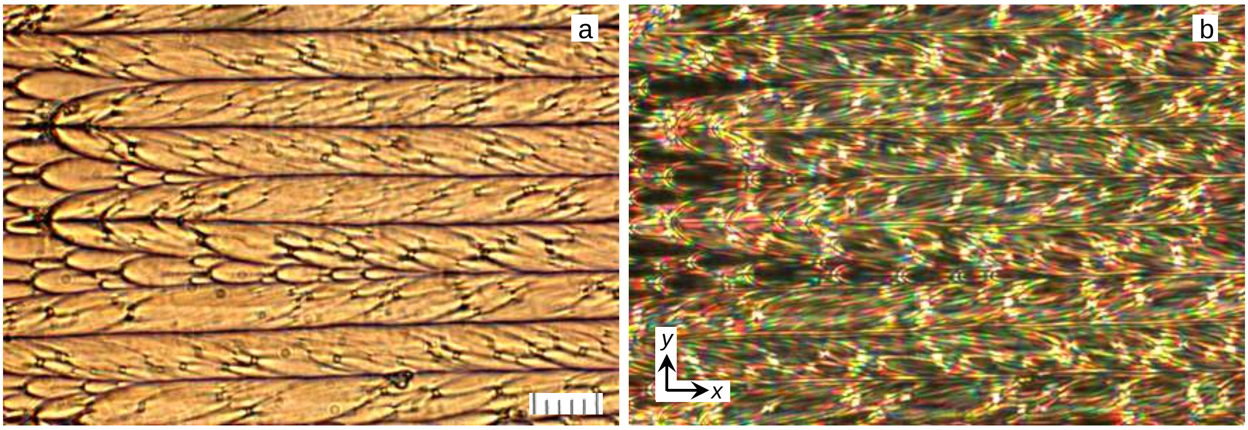

Fig. D4. N_{TB} *phase in CB7CB at ~1°C below the setting point showing two sets of elongated FCDs oppositely inclined by ~15° relative to the rubbing direction; the long horizontal (a) dark and (b) bright periodic lines are the grain boundaries or domain walls involving edge dislocations. (a) P(0), (b) P(0)-A(90). d=20µm. ΔT~0.8 °C. Scale: 5 µm/div.*

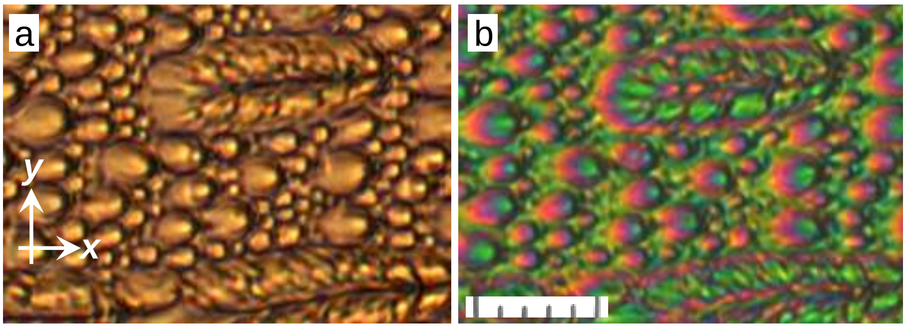

Fig. D5. *The NTB phase of CB7CB supercools to exhibit here the FCD texture at room temperature. d=20 µm. (a) P(0), (b) P(45)-A(135). Scale: 5 µm/div.*

Reference

1. K. S. Krishnamurthy, P. Kumar, N. B. Palakurthy, C. V. Yelamaggad and E. G. Virga, *Soft Matter*, 2016, **12**, 4967.